IOP Publishing | Institute of Physics and Engineering in Medicine Physiological Measurement

Physiol. Meas. **35** (2014) 429–439 doi:10.1088/0967-3334/35/3/429

Removal of artifacts in knee joint vibroarthrographic signals using ensemble empirical mode decomposition and detrended fluctuation analysis

Yunfeng Wu, Shanshan Yang, Fang Zheng, Suxian Cai, Meng Lu and Meihong Wu

School of Information Science and Technology, Xiamen University,
422 Si Ming South Road, Xiamen, Fujian, 361005, People's Republic of China

E-mail: y.wu@ieee.org

Received 18 May 2013, revised 14 January 2014
Accepted for publication 14 January 2014
Published 12 February 2014

Abstract

High-resolution knee joint vibroarthrographic (VAG) signals can help physicians accurately evaluate the pathological condition of a degenerative knee joint, in order to prevent unnecessary exploratory surgery. Artifact cancellation is vital to preserve the quality of VAG signals prior to further computer-aided analysis. This paper describes a novel method that effectively utilizes ensemble empirical mode decomposition (EEMD) and detrended fluctuation analysis (DFA) algorithms for the removal of baseline wander and white noise in VAG signal processing. The EEMD method first successively decomposes the raw VAG signal into a set of intrinsic mode functions (IMFs) with fast and low oscillations, until the monotonic baseline wander remains in the last residue. Then, the DFA algorithm is applied to compute the fractal scaling index parameter for each IMF, in order to identify the anti-correlation and the long-range correlation components. Next, the DFA algorithm can be used to identify the anti-correlated and the long-range correlated IMFs, which assists in reconstructing the artifact-reduced VAG signals. Our experimental results showed that the combination of EEMD and DFA algorithms was able to provide averaged signal-to-noise ratio (SNR) values of 20.52 dB (standard deviation: 1.14 dB) and 20.87 dB (standard deviation: 1.89 dB) for 45 normal signals in healthy subjects and 20 pathological signals in symptomatic patients, respectively. The combination of EEMD and DFA algorithms can ameliorate the quality of VAG signals with great SNR improvements over the raw signal, and the results were also superior to those achieved by wavelet matching pursuit decomposition and time-delay neural filter.

Keywords: knee joint, vibroarthrographic signal, artifact removal, ensemble empirical mode decomposition, detrended fluctuation analysis

(Some figures may appear in colour only in the online journal)

1. Introduction

The knee joint is a type of synovial joint, and also the largest and most complex joint in the human body (Wu *et al* 2010). The articular surface of the knee joint is surrounded by a synovial capsule. The synovial membrane located in the inner layer of the capsule produces the synovial fluid that helps lubricate the joint without any friction. Articular cartilage that pads the ends of the articulation bones can cushion the impact of the knee during locomotion and bounce activities (Wu *et al* 2010). Although the knee joint is able to tolerate moderate stress, it is still often injured in strenuous exercise, especially in sports activities.

Magnetic resonance imaging (MRI), computed tomography (CT), x-ray and arthroscopy are the most frequently used medical techniques for the detection of knee joint pathologies. The imaging-based tools can provide anatomical images of the articular cartilage with relatively good resolution, but they fail to characterize the functional integrity of the cartilage. Arthroscopy is a semi-invasive surgical procedure that may be used to inspect the interior of a knee joint through a small incision (Frank *et al* 1990). However, a knee joint cannot afford repeated examinations or follow-up studies with arthroscopic surgery, because the frequently inspected incision is susceptible to bacterial infection (Rangayyan and Wu 2008).

Vibration arthrometry can be used as an alternative noninvasive technology for the screening of knee joint pathology in clinical practice (Krishnan and Rangayyan 2000, Tanaka and Hoshiyama 2012). The knee joint vibroarthrographic (VAG) signal emitted from a knee joint during flexion (bending) or extension (straightening) movements provides useful information about the functional integrity of the articular cartilage (McCoy *et al* 1987, Rangayyan and Wu 2009). The analysis of VAG signals can extract dominant features associated with degeneration conditions of the degenerative articular cartilage (Rangayyan and Wu 2008, 2009, 2010, Wu and Krishnan 2011, Rangayyan *et al* 2013, Cai *et al* 2013). The removal of artifacts in VAG signals is an essential procedure prior to further quantitative study of pathological features. Baseline wander and random noise are two types of common artifacts in inherent nonstationary VAG signals (Wu *et al* 2013a). Baseline wander usually occurs when the subject performs flexion or extension movements during the VAG signal recording. Random noise can be caused due to the thermal effect in the instrumentation amplifiers and the recording system. The aim of the present study is to combine the ensemble empirical mode decomposition (EEMD) and detrended fluctuation analysis (DFA) methods to eliminate the artifacts in terms of baseline wander and random noise in VAG signals. The DFA algorithm measures the fluctuations in the intrinsic mode functions (IMFs) produced by the EEMD. The baseline wander and random noise can be effectively identified in the IMFs according to the fractal scaling index parameter, and then removed in the reconstructed signals.

2. Signal acquisition

The VAG signals were recorded from 45 healthy adults (age: 30.6 $\pm$ 7.1 yr; body mass index: 20.64 $\pm$ 2.34 kg m^{-2}) and 20 symptomatic patients (age: 35.3 $\pm$ 12.1 yr; body mass index: 21.96 $\pm$ 2.33 kg m^{-2}) with different pathological conditions in their knees. The results of

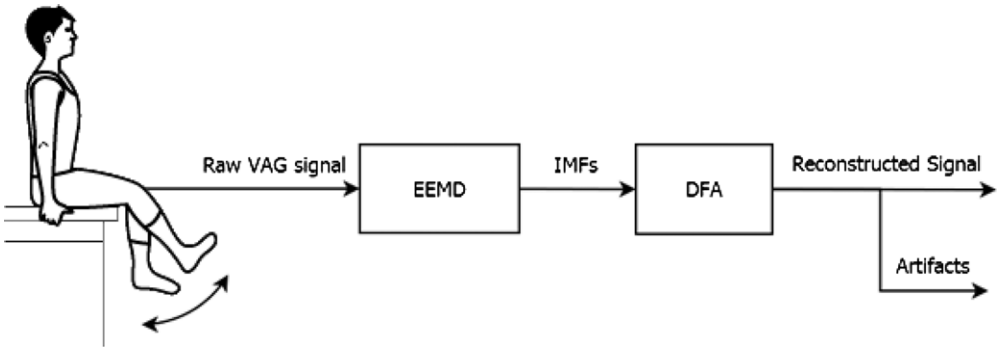

Figure 1. Illustration of the knee joint vibroarthrographic (VAG) signal processing procedure. EEMD: ensemble empirical mode decomposition; IMFs: intrinsic mode functions; DFA: detrended fluctuation analysis.

the two-sample Kolmogorov–Smirnov (KS) test suggested that neither age ($p = 0.4$) nor body mass index ($p = 0.06$) were statistically different between the healthy subjects and symptomatic patients. The healthy subjects were free of muscular or movement disorders, and identified as normal by physical examinations. The patients who had symptoms of patellar and tibial chondromalacia, ligament injury and meniscal tearing were scheduled to undergo arthroscopy examinations or MRI scanning independent of the VAG signal acquisition. The VAG signal data analyzed in the present work were selected from a data set that has been used in our previous related studies (Rangayyan and Wu 2008, 2009, 2010, Rangayyan *et al* 2013, Wu and Krishnan 2011). The other 24 signals of the original 89 VAG data set were not considered in the current work due to the lack of sufficient details about the knee joint pathological conditions. The experimental protocol was approved by the Conjoint Health Research Ethics Board of the University of Calgary (Rangayyan and Wu 2008).

In the signal acquisition procedure, the subjects were asked to sit on a rigid table with the legs freely suspended in the air. Each VAG signal was measured with a miniature accelerometer (Model 3115A, Dytran Instruments, Inc., Chatsworth, CA, USA) placed at the middle-patella position using two-sided adhesive tape when the subject voluntarily swung the leg over an angle range from 135° to 0° (extension movement), and back to 135° (flexion movement) within 4 s (Rangayyan *et al* 1997). The raw signals sampled at 2 kHz were amplified using a universal amplifier (Model 13-4615-18, Gould Instrument Systems, Inc., Cleveland, OH, USA) with a bandwidth of 10 Hz–1 kHz, and then digitized using the LabVIEW software (National Instruments, Austin, TX, USA) with a 12-bit resolution per sample. Auscultation of the knee joint was also performed using an electro-stethoscope. A qualitative description of sound intensity was recorded, together with the relationship to the joint angle. The signal processing experiments and the statistical analysis of the present study were performed with Matlab R2011b (The MathWorks, Inc.).

3. Methods

The work flow of the VAG signal processing procedure implemented in the present work is shown in figure 1. Each raw VAG record is first processed by the EEMD into several IMFs. The DFA algorithm is then applied to identify the inherent correlation property of each IMF. Finally, the IMFs that contain dominant artifacts of baseline wander and random noise are removed to produce the reconstructed artifact-reduced signal. The details of the signal processing procedure are described in the following section.

3.1. Ensemble empirical mode decomposition

Empirical mode decomposition (EMD) was introduced by Huang *et al* (1998) as an effective approach for the analysis of nonlinear and nonstationary signals. The EMD method works by sifting a given signal into a set of IMFs that represent the fast and slow oscillations in the signal (Huang *et al* 1999). For each IMF, the local maxima are all positive and the local minima are all negative (Wu *et al* 2012). The mean values of the upper and lower envelopes of each IMF should be zero. For a signal that is composed of two or more spectral components, the EMD method has the capability to separate these components with different amplitude levels in the decomposed IMFs, as confirmed in the work of Rilling and Flandrin (Rilling and Flandrin 2008). However, the effectiveness of the EMD method is limited by the mode mixing effect (Huang *et al* 2003). Mode mixing is a phenomenon whereby the oscillations with disparate time scales are preserved in one IMF, or where the oscillations with the same time scale are sifted into different IMFs.

Recently, Wu and Huang (2009) proposed a noise-assisted EMD algorithm, named EEMD, to overcome the mode mixing obstacle. The EEMD adds different series of white noise into the signal in several trials. The added white noise plays a crucial role in the decomposition process, because it provides uniformly distributed references of different scales (Wu and Huang 2004). In each trial, the added noise is different, so that the decomposed IMFs have no correlation with the corresponding IMFs from one trial to another. If the number of trials is sufficient, the added noise can be canceled out by ensemble averaging of the corresponding IMFs obtained in the different trials. The details of the EEMD process are described as follows (Wu and Huang 2009).

(i) In the nth trial, a white noise time series $u_n(t)$ is added to a given signal $x(t)$, to attain a new time series $y_n(t) = x(t) + u_n(t)$, for $n = 1, 2, \ldots, N$, where N denotes the ensemble number.

(ii) The noise-contaminated signal $y_n(t)$ is decomposed into a set of IMFs using the original EMD method (Huang *et al* 1998), that is

$$y_n(t) = \sum_{j=1}^{i} c_j^n + r_i^n, \tag{1}$$

where i is the total number of the IMFs in each decomposition, c_j^n is the jth IMF, and r_i^n represents the residue of $y_n(t)$ in the nth trial. To ensure that the number of IMFs in each decomposition is equal, we set a fixed sifting number of 10, to produce each IMF in the present VAG signal decomposition experiments.

(iii) The above two steps are repeated for N trials, with different white noise series $u_n(t)$ added each time.

(iv) The corresponding jth IMFs obtained in the total N trials are averaged, that is

$$c_j^{\text{ave}} = \frac{1}{N} \sum_{n=1}^{N} c_j^n, \tag{2}$$

where c_j^{ave} is the final IMF of the EEMD.

The effectiveness of the EEMD method depends on the appropriate setting of the ensemble number and the amplitude of added noise. According to Wu and Huang (2009), the ensemble number, N, and the amplitude of added noise, A, should satisfy the following rule:

$$\varepsilon = \frac{A}{\sqrt{N}}, \tag{3}$$

where ε represents the final standard deviation of error, which indicates the difference between the original data and the sum of the IMFs obtained with the EEMD.

In our experiments, the standard deviation of the added noise was set to be 0.2 times the standard deviation of the raw VAG signal. The ensemble number was fixed at $N = 100$ to average the corresponding IMFs obtained in the total 100 trials of the EEMD.

3.2. Fractal scaling index

With the IMFs obtained by the EEMD method, we utilized the DFA algorithm to analyze the correlation properties (for example, anti-correlated or long-range correlated) of each decomposed IMF, in terms of the fractal scaling index, in order to identify whether an IMF contained the dominant artifacts in the knee joint VAG signal tested. The fractal scaling index is a parameter that measures the subtle fluctuations associated with intrinsic correlations of the dynamics in a time series. The fractal scaling index can be computed with the DFA algorithm, which is commonly used to determine the statistical self-affinity of the signal tested (Peng *et al* 1992, 1995). The DFA algorithm is popular for the detection of nonstationary time series that exhibit long-range correlation properties (Bak *et al* 1987).

Given an L-length decomposed IMF $c_j^{\text{ave}}(l)$ with the mean value of w_j, the integrated IMF time series $s(m)$ is defined by

$$s(m) = \sum_{l=1}^{m} \left[c_j^{\text{ave}}(l) - w_j \right]. \tag{4}$$

Next, the integrated time series $s(m)$ is divided into several window segments of equal size k, and a least-squares line (i.e., the local linear trend), denoted as $s_k(m)$, that fits the window samples. The local detrended fluctuation is then computed by subtracting the local linear trend $s_k(m)$ from the integrated time series $s(m)$ in each window segment. The averaged fluctuation $F(k)$ is computed with the root-mean-square of the local detrended fluctuations as

$$F(k) = \left[\frac{1}{L} \sum_{m=1}^{L} [s(m) - s_k(m)]^2 \right]^{\frac{1}{2}}. \tag{5}$$

In the present work, the averaged fluctuation computation is repeated over the time scales defined by the window sizes in the range from 10 to 250, with an increment of 20, for each decomposed IMF of 8000 samples in length. The function relating the averaged fluctuation $F(k)$ to the window size k is then represented on a double logarithmic graph. The fractal scaling index, represented as α, denotes the slope of the linear relationship between $\log_{10} F(k)$ and $\log_{10} k$, which is expressed by a power law as $F(k) \sim k^{\alpha}$ (Peng *et al* 1995). For $0.5 < \alpha < 1$, the integrated and detrended time series possess persistent long-range power-law correlations, whereas $0 < \alpha < 0.5$ indicates an anti-correlated property of the time series (Kantelhardt *et al* 2001). Typically, the integrated and detrended time series correspond to white noise when $\alpha = 0.5$, pink noise ($1/f$ noise) when $\alpha = 1$ or brown noise when $\alpha = 1.5$ (Peng *et al* 1992).

4. Results and discussion

Figure 2 displays the IMFs decomposed from the VAG signal of a patient who suffers from anterior cruciate ligament (ACL) and chondromalacia. The EEMD successively produced the 11 IMFs in the decomposition iterations, leaving the residue component as the monotonic trend. It can be observed that different IMFs reveal different degrees of dynamics involved in the raw VAG signal. The IMFs decomposed at the low levels (C1–C3) contained fast (high-frequency) oscillations, and the IMFs decomposed at the higher levels (C4–C11) included

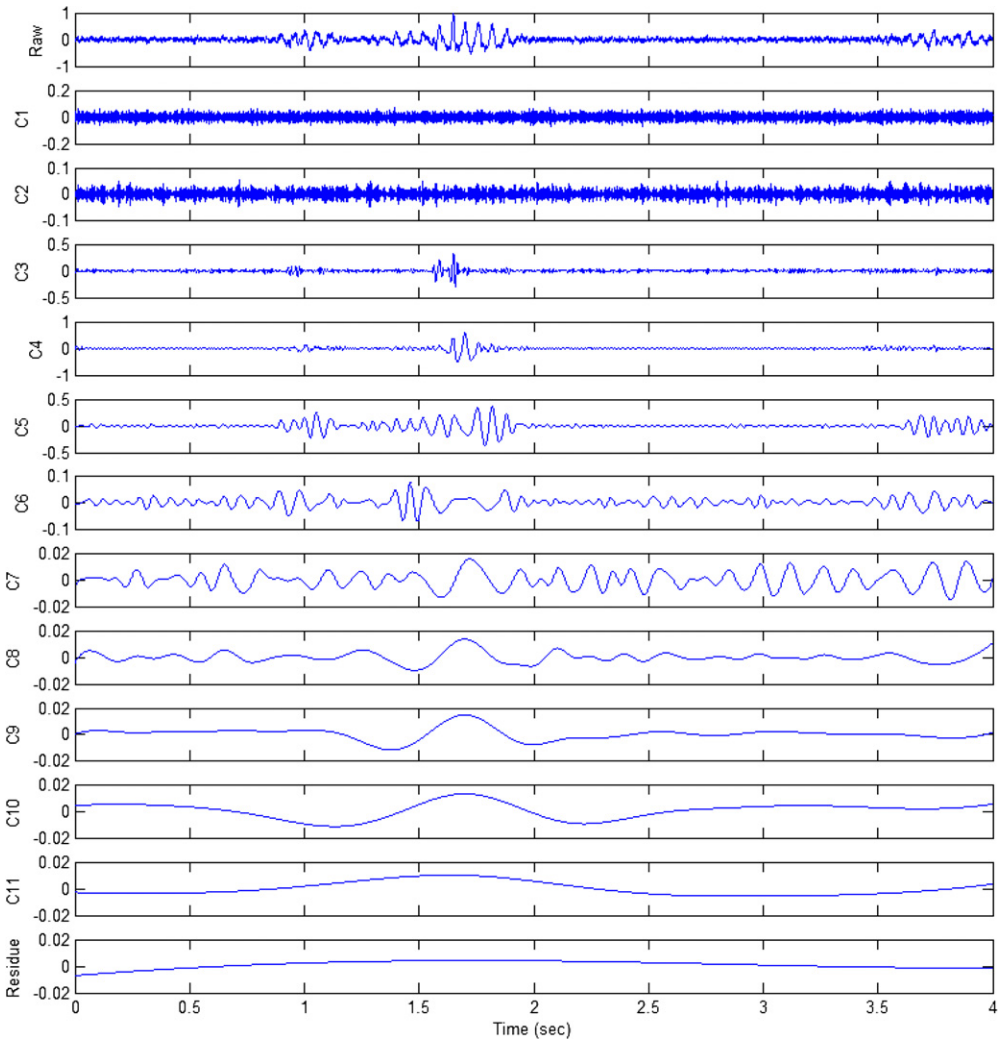

Figure 2. Plots of the IMFs decomposed by the EEMD from the VAG signal of a subject with ACL and chondromalacia. From top to bottom: the raw signal, the corresponding IMFs and the monotonic trend (residue).

more slow (low-frequency) oscillations. The envelopes of the C1 and C2 IMFs were very flat, and did not present the distinct morphological characteristics associated with the pathological conditions of ACL (0.9–1.1 s and 3.7–4 s) and chondromalacia (1.4–1.9 s).

As described in the previous section, we implemented the DFA algorithm to compute the fractal scaling index parameter for each IMF, in order to identify the artifact components in the VAG signal. Figure 3 shows the double-logarithmic relationship between the averaged fluctuation and the window size for the C1, C6 and C8 IMFs displayed in figure 2. It is clear that the three IMFs possess different fractal scaling index values (the slope of the linear fitting in the root-mean-square sense). The fractal scaling index α of the C1 IMF is equal to 0.14, which indicates that this IMF has a large number of anti-correlated components. The C6 and C8 IMFs are both long-range correlated time series ($\alpha > 1.5$). The C8 IMF ($\alpha = 1.86$) contains

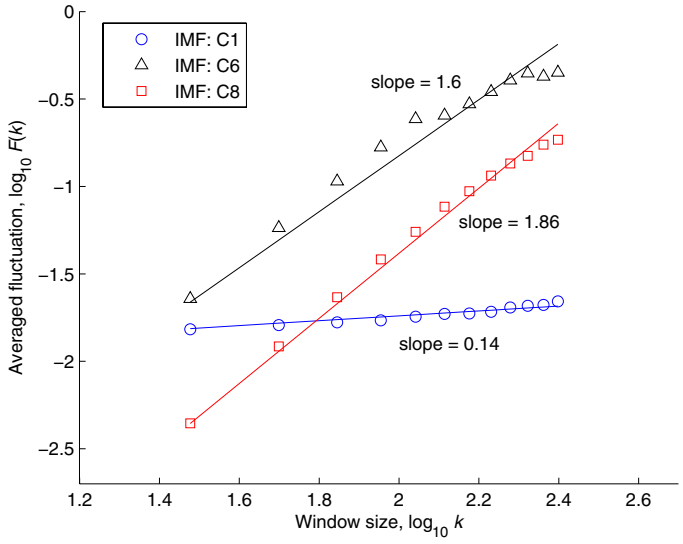

Figure 3. Double logarithmic plots of the linear relationship between averaged fluctuation $F(k)$ and the window size k, for the IMFs C1, C6 and C8, decomposed from the VAG signal shown in figure 2.

more long-range power-law correlated components than the C6 IMF ($\alpha = 1.6$), because the C8 IMF has slower oscillations.

In the present study, we removed the IMFs with anti-correlations ($0 < \alpha < 0.5$) and monotonic residue (baseline wander), and reconstructed each VAG signal with the long-range correlated IMFs ($\alpha > 0.5$). Figure 4 shows the reconstructed artifact-reduced signal, in comparison with the artifacts and the raw VAG signal. It can be observed that the high-frequency noise and baseline wander have been reduced, and the morphological patterns in the VAG signal were not distorted. It is also worth noting that some rapidly varying components still exist in the reconstructed VAG signal in figure 4. The components are identified to be long-range correlated, which implies that such components are not random noise but generated by some type of physiological process. We assume that these components are the mechanomyographic and vibromyographic responses of the superficial muscles contracted during the leg swing in the signal acquisition procedure.

Table 1 gives the SNR results obtained by the wavelet matching pursuit (MP) decomposition (Krishnan and Rangayyan 2000), the time-delay neural filter (Wu *et al* 2013a) and the combination of EEMD and DFA algorithms. The statistical values demonstrate that all three methods have good averaged performance for artifact removal in VAG signals, because the three methods made SNR improvements larger than 9 dB for both normal and pathological signals. Both the time-delay neural filter and the combination of EEMD and DFA algorithms provided SNR values reaching over 20 dB, much better than the wavelet MP decomposition. For the best signal case, the combination of EEMD and DFA algorithms produced an SNR value of 24.93 dB, slightly lower than that of the time-delay neural filter. However, for both normal and pathological signals, the SNR standard deviation values of the combination of EEMD and DFA algorithms were much smaller than those of the time-delay neural filter. We also applied the two-sample KS test to evaluate whether the combination of EEMD and DFA algorithms outperformed the time-delay neural filter in a statistical sense. For both the

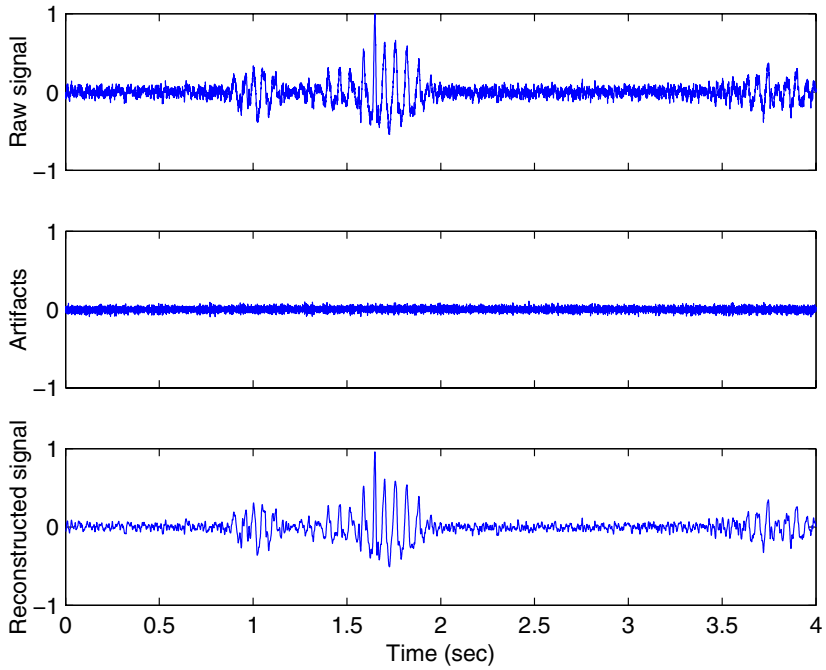

Figure 4. Illustration of the artifact reduction effect for the VAG signal of the patient with ACL and chondromalacia shown in figure 2: (a) the raw signal, (b) the artifacts removed, and (c) the reconstructed artifact-reduced signal.

Table 1. Signal-to-noise ratio (SNR) results in dB of the processed knee joint vibroarthrographic (VAG) signals obtained by the combination of the EEMD and DFA methods, in comparison with the wavelet matching pursuit (MP) decomposition and the time-delay neural filter presented in previous studies (Krishnan and Rangayyan 2000, Wu *et al* 2013a). Statistical values are mean ± standard deviation.

	SNR			
	Normal signals ($n = 45$)	Pathological signals ($n = 20$)	Worse case	Best case
Raw VAG signals	5.49 ± 2.59	5.5 ± 3.1	0.53	14.63
Wavelet MP decomposition (Krishnan and Rangayyan 2000)	14.97 ± 6.4	16.42 ± 5.76	7.92	22.19
Time-delay neural filter (Wu *et al* 2013a)	20.4 ± 6.18	20.64 ± 4.96	14.13	25.35
EEMD+DFA	20.52 ± 1.14[a]	20.87 ± 1.89[a]	16.71	24.93

[a] The results of the two-sample Kolmogorov–Smirnov test indicated that the SNR values obtained by the EEMD and DFA methods were significantly different ($p < 0.001$) from those of the time-delay neural filter for both normal and pathological VAG signals.

normal and pathological VAG signal groups, the p values ($p < 0.001$) given by the KS test showed that the SNR values obtained by the combination of EEMD and DFA methods were significantly different from those of the time-delay neural filter. Such results indicated that the combination of EEMD and DFA algorithms achieved a more stable performance for most of

the VAG signals than the time-delay neural filter, indicating that the combination of EEMD and DFA algorithms described in the present work could be better suited for the artifact removal task in VAG signal processing.

5. Conclusion remarks

Imaging modalities such as Magnetic resonance imaging (MRI), computed tomography (CT) and x-ray are currently prevailing in knee joint disorder detection. X-ray and CT are better for joint space narrowing, osteophytes and subchondral bone sclerosis because articular cartilage does not have a high density in contrast to bone. MRI is more sensitive to defects of articular cartilage surfaces, but it is not very well suited to characterizing the softening, stiffness or fissuring conditions of cartilage (Wu *et al* 2010). Ultrasound imaging is extremely sensitive in the detection of soft tissue changes in osteoarthritic joints, and it helps rheumatologists to establish guidelines for the assessment of abnormalities in articular cartilage, bony cortex and synovial tissue (Möller *et al* 2008). However, the ultrasonic visualization of articular cartilage is restricted by the acoustic windows, whose width is determined by the anatomy of the joint tested, because the ultrasound beam is not able to penetrate bony cortex (Möller *et al* 2008). As a recently developed infrared-based imaging technique, optical coherence tomography also demonstrated some merits in osteoarthritis detection, by providing *in vivo* cartilage images at a resolution of micrometers (Li *et al* 2005, Rashidifard *et al* 2013). Standardized scanning guidelines based on more clinical trials are necessary to explore the potential of optical coherence tomography in monitoring osteoarthritis progression. On the other hand, recent studies (Li and Herzog 2006, Kiviranta *et al* 2008) have shown that the early onset of cartilage degeneration may occur prior to any visible change on the articular surface. Quantitative mechanical evaluation using a handheld indentation probe during knee arthroscopy has been introduced to detect irreversible early degenerative changes in articular cartilage tissue (Li and Herzog 2006, Kiviranta *et al* 2008). Recent related work suggested that the indenter geometry and its porosity would produce different deformation properties in cartilage, and may affect the precise evaluation of cartilage degeneration (Li and Herzog 2006). In addition, the arthroscopic incision is more susceptible to infection, which limits the use of knee arthroscopy for repeated examinations after surgery. As a noninvasive method, knee joint vibroarthrography is also useful for point-of-care monitoring of articular cartilage disorders by using miniature accelerometers and a portable signal acquisition board (Rangayyan and Wu 2009, 2010, Wu and Krishnan 2011, Rangayyan *et al* 2013, Cai *et al* 2013). However, the vibroarthrographic (VAG) signals are often contaminated with white noise and baseline wander during signal acquisition experiments, which affect the signal quality and pathological assessment. Digital signal processing plays an important role in VAG signal analysis, because artifact-free signals with high resolutions could help physicians better diagnose knee joint pathologies (Cai *et al* 2012). In addition, with the distinct features extracted from the VAG signals, computational algorithms can be effectively used for screening the pathological abnormalities from the normal signals (Wu and Krishnan 2009a, 2009b, Wu *et al* 2013b). This paper presents a novel approach that combines ensemble empirical mode decomposition (EEMD) and detrended fluctuation analysis (DFA) algorithms for artifact removal in VAG signals. The EEMD method is able to decompose different intrinsic mode functions (IMFs) with fast and low oscillations in the raw VAG signal. Next, the DFA algorithm can be used to identify the anti-correlated and the long-range correlated IMFs, which helps reconstruct the artifact-reduced VAG signals. The signal-to-noise ratio results in the statistical sense demonstrated that the combination of EEMD and DFA algorithms outperformed either the wavelet matching pursuit decomposition or the

time-delay neural filter. Future work will emphasize the quantitative study of the morphological features of VAG signals related to pathological conditions in degenerative knee joints.

Acknowledgments

The authors would like to thank Dr Rangaraj M Rangayyan, Dr Cyril B Frank and Dr Gordon D Bell for the data acquisition work. This study was supported in part by the National Natural Science Foundation of China (grant no 81101115 and 31200769), the Natural Science Foundation of Fujian Province of China (grant number 2011J01371) and the Fundamental Research Funds for the Central Universities of China (grant number 2010121061). Dr Junfeng Wu was also supported by the 2013 Program for New Century Excellent Talents in Fujian Province University.

References

Bak P, Tang C and Wiesenfeld K 1987 Self-organized criticality: an explanation of the $1/f$ noise *Phys. Rev. Lett.* **59** 381–4

Cai S X, Wu Y F, Xiang N, Zhong Z T, He J, Shi L and Xu F 2012 Detrending knee joint vibration signals with a cascade moving average filter *Proc. of IEEE 34th Annu. Int. Conf. of Engineering in Medicine and Biology Society* pp 4357–60

Cai S X, Yang S S, Zheng F, Lu M, Wu Y F and Krishnan S 2013 Knee joint vibration signal analysis with matching pursuit decomposition and dynamic weighted classifier fusion *Comput. Math. Methods Med.* **2013** 904267

Frank C B, Rangayyan R M and Bell G D 1990 Analysis of knee sound signals for non-invasive diagnosis of cartilage pathology *IEEE Eng. Med. Biol. Mag.* **9** 65–8

Huang N E, Shen Z and Long S R 1999 A new view of nonlinear water waves: the Hilbert spectrum *Annu. Rev. Fluid Mech.* **31** 417–57

Huang N E, Shen Z, Long S R, Wu M C, Shih H H, Zheng Q, Yen N C, Tung C C and Liu H H 1998 The empirical mode decomposition and the Hilbert spectrum for nonlinear and non-stationary time series analysis *Proc. R. Soc.* A **454** 903–95

Huang N E, Wu M L C, Long S R, Shen S S P, Qu W, Gloersen P and Fan K L 2003 *Proc. R. Soc.* A **459** 2317–45

Kantelhardt J W, Koscielny-Bunde E, Rego H H, Havlin S and Bunde A 2001 Detecting long-range correlations with detrended fluctuation analysis *Physica* A **295** 441–54

Kiviranta P, Lammentausta E, Töyräs J, Kiviranta I and Jurvelin J S 2008 Indentation diagnostics of cartilage degeneration *Osteoarthritis Cartilage* **16** 796–804

Krishnan S and Rangayyan R M 2000 Automatic de-noising of knee-joint vibration signals using adaptive time-frequency representations *Med. Biol. Eng. Comput.* **38** 2–8

Li L P and Herzog W 2006 Arthroscopic evaluation of cartilage degeneration using indentation testing–influence of indenter geometry *Clin. Biomech.* **21** 420–6

Li X, Martin S, Pitris C, Ghanta R, Stamper D L, Harman M, Fujimoto J G and Brezinski M E 2005 High-resolution optical coherence tomographic imaging of osteoarthritic cartilage during open knee surgery *Arthritis Res. Therapy* **7** R318–23

McCoy G F, McCrea J D, Beverland D E, Kernohan W G and Mollan R A B 1987 Vibration arthrography as a diagnostic aid in diseases of the knee: a preliminary report *J. Bone Joint Surg. Br.* **69** 288–93

Möller I, Dong D, Naredo E, Filippucci E, Carrasco I, Moragues C and Iagnocco A 2008 Ultrasound in the study and monitoring of osteoarthritis *Osteoarthritis Cartilage* **16** S4–7

Peng C K, Buldyrev S V, Goldberger A L, Havlin S, Sciortino F, Simons M and Stanley H E 1992 Long-range correlations in nucleotide sequences *Nature* **356** 168–70

Peng C K, Havlin S, Stanley H E and Goldberger A L 1995 Quantification of scaling exponents and crossover phenomena in nonstationary heartbeat time series *Chaos* **5** 82–7

Rangayyan R M, Krishnan S, Bell G D, Frank C B and Ladly K O 1997 Parametric representation and screening of knee joint vibroarthrographic signals *IEEE Trans. Biomed. Eng.* **44** 1068–74

Rangayyan R M, Oloumi F, Wu Y F and Cai S X 2013 Fractal analysis of knee-joint vibroarthrographic signals via power spectral analysis *Biomed. Signal Process. Control* **8** 26–9

Rangayyan R M and Wu Y F 2008 Screening of knee-joint vibroarthrographic signals using statistical parameters and radial basis functions *Med. Biol. Eng. Comput.* **46** 223–32
Rangayyan R M and Wu Y F 2009 Analysis of vibroarthrographic signals with features related to signal variability and radial-basis functions *Ann. Biomed. Eng.* **37** 156–63
Rangayyan R M and Wu Y F 2010 Screening of knee-joint vibroarthrographic signals using probability density functions estimated with Parzen windows *Biomed. Signal Process. Control* **5** 53–8
Rashidifard C, Vercollone C, Martin S, Liu B and Brezinski M E 2013 The application of optical coherence tomography in musculoskeletal disease *Arthritis* **2013** 563268
Rilling G and Flandrin P 2008 One or two frequencies? The empirical mode decomposition answers *IEEE Trans. Signal Process.* **56** 85–95
Tanaka N and Hoshiyama M 2012 Vibroarthrography in patients with knee arthropathy *J. Back Musculoskeletal Rehabil.* **25** 117–22
Wu Y F and Krishnan S 2009a Classification of knee-joint vibroarthrographic signals using time-domain and time-frequency domain features and least-squares support vector machine *Proc. of the 16th Int. Conf. on Digital Signal Processing* pp 361–6
Wu Y F and Krishnan S 2009b An adaptive classifier fusion method for analysis of knee-joint vibroarthrographic signals *Proc. of 2009 Int. Conf. on Computational Intelligence for Measurement Systems and Applications* pp 190–3
Wu Y F and Krishnan S 2011 Combining least-squares support vector machines for classification of biomedical signals: a case study with knee-joint vibroarthrographic signals *J. Exp. Theor. Artif. Intell.* **23** 63–77
Wu Y F, Cai S X, Xu F, Shi L and Krishnan S 2012 Chondromalacia patellae detection by analysis of intrinsic mode functions in knee joint vibration signals *IFMBE Proc. of 2012 World Congress on Medical Physics and Biomedical Engineering* vol 39 pp 493–6
Wu Y F, Cai S X, Lu M, Yang S S, Zheng F, Xiang N, He J and Zhong Z T 2013a Noise cancellation in knee joint vibration signals using a time-delay neural filter and signal power error minimization method *J. Convergence Inform. Technol.* **8** 912–9
Wu Y F, Cai S X, Yang S S, Zheng F and Xiang N 2013b Classification of knee joint vibration signals using bivariate feature distribution estimation and maximal posterior probability decision criterion *Entropy* **15** 1375–87
Wu Y F, Krishnan S and Rangayyan R M 2010 Computer-aided diagnosis of knee-joint disorders via vibroarthrographic signal analysis: a review *Crit. Rev. Biomed. Eng.* **38** 201–24
Wu Z H and Huang N E 2004 A study of the characteristics of white noise using the empirical mode decomposition method *Proc. R. Soc.* A **460** 1597–611
Wu Z H and Huang N E 2009 Ensemble empirical mode decomposition: a noise-assisted data analysis method *Adv. Adapt. Data Anal.* **1** 1–41